

# Looking for simple correction functions between the mean radiant temperature from the “standard black globe” and the “six-directional” techniques in Taiwan

Noémi Kántor · Attila Kovács · Tzu-Ping Lin

Received: 31 December 2013 / Accepted: 22 June 2014 / Published online: 20 July 2014  
© Springer-Verlag Wien 2014

**Abstract** Mean radiant temperature ( $T_{\text{mrt}}$ ) values were calculated and compared to each other in Taiwan based on the six-directional and globe techniques. In the case of the six-directional technique (measurements with pyranometers and pyrgeometers), two different  $T_{\text{mrt}}$  values were calculated: one representing the radiation load on a standing man [ $T_{\text{mrt}}(\text{st})$ ] and the other which refers to a spherical reference shape [ $T_{\text{mrt}}(\text{sp})$ ]. Moreover,  $T_{\text{mrt}}(T_g)$  was obtained through the globe thermometer technique applying the standard black globe. Comparing  $T_{\text{mrt}}$  values based on the six-directional technique but with different reference shapes revealed that the difference was always in the  $\pm 5$  °C domain. Of the cases, 75 % fell into the  $\pm 5$  °C Delta  $T_{\text{mrt}}$  range when we compared different techniques with similar reference shapes [ $T_{\text{mrt}}(\text{sp})$  and  $T_{\text{mrt}}(T_g)$ ] and only 69 % when we compared the different techniques with different reference shapes [ $T_{\text{mrt}}(\text{st})$  and  $T_{\text{mrt}}(T_g)$ ]. Based on easily accessible factors, simple correction functions were determined to make the  $T_{\text{mrt}}(T_g)$  values of already existing outdoor thermal comfort databases comparable with other databases which involve sixdirectional  $T_{\text{mrt}}$ . The corrections were conducted directly between the  $T_{\text{mrt}}(T_g)$  and  $T_{\text{mrt}}(\text{sp})$  values and also indirectly, i.e., by using the values of  $T_g$  to reduce the differences between  $T_{\text{mrt}}(\text{sp})$  and  $T_{\text{mrt}}(T_g)$ . Both correction

methods resulted in considerable improvement and reduced the differences between the  $T_{\text{mrt}}(\text{sp})$  and the  $T_{\text{mrt}}(T_g)$  values. However, validations with an independent database from Hungary revealed that it is not suggested to apply the correction functions under totally different background climate conditions.

## 1 Introduction

Human thermal comfort is an issue with emerging importance in the field of human biometeorology in which results should be applied in the practice of urban planning/design process (Mayer 1993; Lin 2009). Thermal conditions of an urban space as well as the way how the people perceive these conditions are highly relevant to their satisfaction, and, as a consequence, they influence the pattern of area usage (Nikolopoulou et al. 2001; Nikolopoulou and Steemers 2003; Thorsson et al. 2004; Nikolopoulou and Lykoudis 2006; Kántor and Unger 2010). Very uncomfortable thermal conditions may cause the avoidance of certain urban spaces, while comfortable microclimate can facilitate the outdoor activity of citizens, including several positive aspects like supporting socialization, stimulating the general well-being and the human health (Nikolopoulou and Lykoudis 2007; Mayer 2008).

Thermal conditions involve the overall effect of four meteorological parameters, namely the air temperature, air humidity, wind velocity, and the so-called mean radiation temperature, which have to be considered together with the level of human activity (metabolism) and the clothing insulation (Fanger 1972; Jendritzky 1993; Mayer 1993, 2008). Many studies have already pointed out that during sunny conditions, the mean radiant temperature ( $T_{\text{mrt}}$  [°C]), which combines the thermal effect of all short- and long-wave radiation fluxes reaching the body into one temperature-unit value (Fanger 1972; VDI 1998), is the main influencing meteorological parameter of thermal comfort (Jendritzky and Nübler 1981; Mayer and Höppe 1987; Mayer

N. Kántor (✉)  
Research Center for the Humanities and Social Sciences,  
National Chung Hsing University, 250 Kuo Kuang Road,  
Taichung 402, Taiwan  
e-mail: sztyepp@gmail.com

A. Kovács  
Department of Climatology and Landscape Ecology,  
University of Szeged, 2 Egyetem Street, Szeged 6722, Hungary

T.-P. Lin  
Department of Architecture, National Cheng Kung University,  
1 University Road, Tainan 701, Taiwan  
e-mail: lin678@gmail.com

1993; Gulyás et al. 2006; Ali-Toudert and Mayer 2007; Mayer et al. 2008; Holst and Mayer 2010; Shashua-Bar et al. 2012; Lee et al. 2013).

### 1.1 Measurement-based $T_{\text{mrt}}$ techniques

$T_{\text{mrt}}$  is defined as the uniform temperature of an imaginary black-radiant enclosure in which the body would exchange the same energy via radiation as in the real non-uniform environment (ASHRAE 2001). The most popular measurement technique used outdoors to determine  $T_{\text{mrt}}$  is the six-directional technique suggested by the VDI 3787 (VDI 1998) which is applied by several research groups (Streiling and Matzarakis 2003; Ali-Toudert 2005; Ali-Toudert et al. 2005; Ali-Toudert and Mayer 2007; Oliveira and Andrade 2007; Thorsson et al. 2007; Andrade et al. 2011; Kántor et al. 2012a, 2012b). Other researchers applied the globe thermometer technique, described in the ISO 7726 (ISO 1985, 1998), because of its affordable price and compact size, especially for multiple-point simultaneous measurement (Chen et al. 2004; Nikolopoulou and Lykoudis 2006, Walton et al. 2007; Hwang and Lin 2007, Hwang et al. 2010, 2011; Lin et al. 2010, 2011; Deb and Ramachandiraiah 2010, 2011; Krüger et al. 2011; Krüger and Rossi 2011; Ng and Cheng 2012; Abdel-Ghany et al. 2013).

#### 1.1.1 Six-directional technique

Up today, the six-directional technique, introduced by Höppe (1992), is considered the most accurate measurement method to obtain  $T_{\text{mrt}}$  values in an outdoor context. According to this technique, short- and long-wave radiation flux densities ( $K_i, L_i$  [ $\text{W}/\text{m}^2$ ]) are measured separately by pyranometers and pyrgeometers from six perpendicular directions ( $i: 1\dots 6$ ), i.e., from the four lateral directions as well as from the upper and lower hemispheres. Using the measured radiation flux densities, the  $T_{\text{mrt}}$  can be calculated as follows:

$$T_{\text{mrt}} = \sqrt[4]{\frac{\sum_{i=1}^6 W_i \cdot (a_k \cdot K_i + a_l \cdot L_i)}{a_l \cdot \sigma}} - 273.15$$

where  $a_k$  and  $a_l$  are the absorption coefficients of the clothed human body in the short- and long-wave radiation domains (with 0.7 and 0.97 suggested values, respectively),  $\sigma$  is the Stefan–Boltzmann constant ( $5.67 \cdot 10^{-8} \text{ W}/\text{m}^2 \text{ K}^4$ ), and  $W_i$  is a directional dependent weighting factor (the sum of the  $W_i$  values needs to be 1).

By assessing different  $W_i$  values to the different directions, the resulted  $T_{\text{mrt}}$  will express the radiation load on different reference shapes. During outdoor thermal comfort/stress investigations, the  $T_{\text{mrt}}$  of a standing human body is in the center of interest. This *standing man*  $T_{\text{mrt}}$ —hereinafter referred to as  $T_{\text{mrt}}(\text{st})$ —can be calculated by using 0.22 as  $W_i$  in the case of

the lateral and 0.06 for the vertical directions (Höppe 1992). Applying 0.167 as  $W_i$  in the case of all six directions, the resulted  $T_{\text{mrt}}$  would represent the radiation load on a *spherical reference shape* (Thorsson et al. 2007)—hereinafter referred to as  $T_{\text{mrt}}(\text{sp})$ . In fact,  $T_{\text{mrt}}(\text{st})$  represents the radiation load on a standing column, and  $T_{\text{mrt}}(\text{sp})$  represents the radiation load on a cube (Kántor et al. 2013).

#### 1.1.2 Globe thermometer technique

The other main technique to determine  $T_{\text{mrt}}$  is based on simultaneous measurements with the so-called globe thermometer, a dry bulb thermometer, and an anemometer. The standard black globe thermometer is actually a thermometer which sensor is in the center of a matt black-painted hollow copper sphere with an emissivity ( $\epsilon$ ) of 0.95, a diameter ( $D_g$ ) of 0.15 m, and a wall thickness of 0.4 mm (Vernon 1930; Bedford and Warner 1934; ISO 1985, 1998).  $T_g$  [ $^{\circ}\text{C}$ ] is the globe temperature measured inside the globe, and its value depends on the radiation and convective heat exchange processes between the globe and the environment. Indeed,  $T_g$  is affected by the atmospheric parameters of  $T_{\text{mrt}}$  (i.e., the short- and long-wave radiation fluxes), the air temperature ( $T_a$  [ $^{\circ}\text{C}$ ]), and the wind velocity ( $v$  [ $\text{m}/\text{s}$ ]). The globe reaches the equilibrium when the radiant and convective heat exchanges are balanced (it takes some time!), and in this case, we can express the value of  $T_{\text{mrt}}$  according to the following:

$$T_{\text{mrt}} = \sqrt[4]{(T_g + 273.15)^4 + \frac{h_{\text{Cg}}}{h_{\text{Rg}}} \cdot (T_g - T_a) - 273.15}$$

where  $h_{\text{Rg}}$  is the coefficient of radiation, and  $h_{\text{Cg}}$  is the coefficient of convection (ISO 1985, 1998). In the case of a given globe, the former has a constant value

$$h_{\text{Rg}} = \epsilon \cdot \sigma$$

while the latter depends on the wind velocity

$$h_{\text{Cg}} = 6.3 \cdot \frac{v^{0.6}}{D_g^{0.4}}$$

(The  $v$  is in meter/second, and the globe's diameter is in meter units!)

After substituting the parameters regarding the standard black globe, the  $T_{\text{mrt}}$  can be calculated according to the following equation (ISO 1985, 1998):

$$T_{\text{mrt}} = \sqrt[4]{(T_g + 273.15)^4 + 2.498 \cdot 10^8 \cdot v^{0.6} \cdot (T_g - T_a) - 273.15}$$

This globe temperature-based  $T_{\text{mrt}}$  value will be referred to hereinafter as  $T_{\text{mrt}}(T_g)$ .

Although the globe technique is more convenient and cheaper than the six-directional method, researchers have already pointed out shortcomings using this technique outdoors. The most important issues can be listed as follows (ASHRAE 2001; Spagnolo and de Dear 2003; Ali-Toudert 2005):

- because of the rapidly variable conditions (radiation and wind field) in outdoors, the globe has no time to reach its equilibrium (the standard black globe needs ca. 15 min),
- because of the shape of the globe, the resulted  $T_{\text{mrt}}$  cannot represent perfectly the radiation load on a standing man,
- because of the black color of the globe, it absorbs too much short-wave radiation compared to the clothed human body.

In spite of these issues, there are lots of already existing outdoor thermal comfort studies including  $T_{\text{mrt}}$  values based on the standard black globe technique (Chen et al. 2004; Walton et al. 2007; Hwang and Lin 2007, Hwang et al. 2010, 2011; Lin et al. 2010, 2011; Abdel-Ghany et al. 2013) or based on measurements with smaller (0.04–0.05 m in diameter) and therefore faster black or gray globes (response time ca. 5–10 min) which fit better to the outdoor conditions (Nikolopoulou and Lykoudis 2006, 2007; Thorsson et al. 2007; Deb and Ramachandraiah 2010, 2011; Krüger et al. 2011; Krüger and Rossi 2011; Ng and Cheng 2012; Abdel-Ghany et al. 2013; Tan et al. 2013, 2014; Pearlmutter et al. 2014). However, the smaller is the globe, the greater is the effect of the convective heat exchange (i.e., air temperature and wind velocity) on the resulted globe temperature, which reduces the accuracy of the  $T_{\text{mrt}}$  calculation (ISO 1985).

To analyze these already existing databases together with others' data in a scientifically sound way,  $T_{\text{mrt}}(T_g)$  values should be compared first with the more reliable six-directional method to determine the differences between the techniques. For example, Thorsson et al. (2007) validated the globe technique via six-directional measurements in Sweden and suggested a modified  $T_{\text{mrt}}(T_g)$  equation to obtain better results (closer to the six-directional  $T_{\text{mrt}}(\text{sp})$  values); however, they used not the standard black globe, but a smaller (0.038 m in diameter), gray-painted acrylic one. Tan et al. (2013) applied their methodological approach to derive a similar equation for the tropical environment of Singapore. Other researchers compared the  $T_{\text{mrt}}$  values resulted from different models (ENVI-met, RayMan, SOLWEIG) to the six-directional  $T_{\text{mrt}}(\text{st})$  (Ali-Toudert 2005; Ali-Toudert and Mayer 2007; Thorsson et al. 2007; Matzarakis et al. 2007, 2010; Andrade and Alcoforado 2008; Lindberg et al. 2008; Lindberg and Grimmond 2011), but none of the studies discussed the details, for example the application limits, or did not suggest possible correction functions between the different techniques based  $T_{\text{mrt}}$  values. This is however an

important issue, as there are many thermal comfort studies and already existing databases in the world which include  $T_{\text{mrt}}$  values based on different techniques. To compare the results and findings of these studies, we should know the differences emerging from the fact that the applied  $T_{\text{mrt}}$  techniques and/or measurement equipments are different.

## 1.2 Goals of the present study

Our most important short-term aim is to facilitate the reliable comparison of already existing outdoor thermal comfort databases (including measured meteorological parameters and calculated bioclimate indices as well as subjective data from questionnaire surveys) collected in Taiwan (Hwang and Lin 2007; Lin et al. 2011) and in Hungary (Kántor et al. 2012a, 2012b). The on-site measurement series in Taiwan included the globe technique with the standard black globe to determine the  $T_{\text{mrt}}$ , while the Hungarian researchers applied six-directional measurements. Therefore, the *first goal* of this paper is to check whether these two techniques result in the same  $T_{\text{mrt}}$  values under the same radiation conditions and quantify what an error can be assumed in terms of  $T_{\text{mrt}}$  and in terms of a bioclimate index when we use the  $T_{\text{mrt}}$  values of both techniques without modification.

The *second goal* is to specify easy correction methods to facilitate the comparison of the globe-based  $T_{\text{mrt}}$  values to the six-directional technique-based  $T_{\text{mrt}}$  values. To achieve the first and second goals, a Taiwanese “Correction Database” of parallel globe–six-directional measurement series will be used.

Our long-term aim is to support the comparison of outdoor thermal comfort databases including different  $T_{\text{mrt}}$  techniques all over the world. Therefore, the *third goal* of this paper is to analyze whether the correction functions derived in Taiwan can be applied in different geographical/climate context or not, i.e., to quantify their efficiency using an independent database (from Hungary) of parallel globe–six-directional measurements.

## 2 Applied databases and analyses

### 2.1 The Taiwanese “correction database”

In accordance with our short-term aim, namely to support the comparison of the already existing Taiwanese thermal comfort database from the years 2005 to 2006 (called field investigation of outdoor thermal comfort (FIOT) project by Lin et al. 2011) including  $T_{\text{mrt}}(T_g)$  to others' data including  $T_{\text{mrt}}(\text{st})$  or  $T_{\text{mrt}}(\text{sp})$ , we use a parallel six-directional and globe thermometer measurement series conducted in Taiwan. In the frame of these measurements, 1-min averages of  $K_i$  and  $L_i$  as well as  $T_g$ ,  $v$ ,  $T_a$

were recorded in the National Formosan University in Huwei (23.7° N, 120.43° E) in the years 2010–2011. The measurement of relative humidity ( $RH$  [%]) was also necessary to be able to calculate later the physiologically equivalent temperature ( $PET$  [°C]; Höppe 1999) bioclimate index with the RayMan model (Matzarakis et al. 2007, 2010). In correspondence with the gravity center of a standing man, the sensors were mounted at 1.1 m above ground level (Mayer and Höppe 1987). The characterization of the instruments is included in Table 1.

The parallel measurement series were carried out in the daylight hours of 12 days. Ten days were on the top of the university without considerable horizon limiting objects (with a sky view factor (SVF) near to 1) and 2 days on the street level. On one of these days, the sensors were shaded partly by the surrounding buildings, while on the other day, they were in the shade of well-developed banyan trees during the whole day. As the motivation was to identify the best and the simplest method to correct the  $T_{mrt}(T_g)$  values of the earlier Taiwanese FIOT project (Hwang and Lin 2007, Lin et al. 2011), we sought to compile a *Correction Database* from the parallel measurements with similar atmospheric/thermal conditions to those recorded during the FIOT.

Based on literature review and the results of earlier studies (Thorsson et al. 2007), as well as on preliminary analyses of the Taiwanese data, global radiation ( $K\downarrow$ ; recorded by the up-facing pyrano meter) and air movement (the nearly zero  $v$  values and the strong gusts) were identified important easily accessible factors which may strongly influence the obtained  $T_{mrt}(T_g)$  values' deviations from the "desired" six-directional  $T_{mrt}$ . The  $K\downarrow$  domain of the FIOT and the Correction Database were quite similar; however, the wind velocity values recorded on the roof during the Correction measurements covered a considerably wider range than those in the FIOT project. To be consistent with the FIOT conditions, we removed all the cases from the Correction Database when the wind velocity was outside the 0.5–3.5-m/s range. (However, because of the cup anemometer's inertia in the case of very slight and very strong

wind and to be able to smooth the fluctuation of  $v$  values and keep longer continuous time periods in the database, this filter was actually based on the 9-min moving averages of  $v$ ).

Furthermore, during the detailed preliminary analysis of the data, we found almost no deviations between the different  $T_{mrt}$  values when the sensors were totally shaded, i.e., when they received no direct radiation for a longer period (left side in Fig. 1). Consequently, the  $T_{mrt}(T_g)$  values do not require modification in these situations, and we need to analyze only the cases with the chance of direct irradiation. Correspondingly, we removed the days when the sensors were shaded by obstacles. After filtering out all of the mentioned cases, our Correction Database includes 3,833 datasets from 9 measurement days. The main descriptive statistics of the basic and calculated parameters which are used in this study are summarized in Table 2.

In line with the first research objective, we will present the differences evolving in outdoor conditions between the two most popular measurement-based  $T_{mrt}$  techniques, i.e., the six-directional technique representing the radiation load of a standing man as well as the black globe technique— $T_{mrt}(st)$  and  $T_{mrt}(T_g)$ . However, in contrast to the earlier studies which compared the  $T_{mrt}(T_g)$  values only directly to the desired  $T_{mrt}(st)$  values, we aim to distinguish the divergences emerging from the different reference shapes (spherical shape vs. standing man shape) as well as from the other issues regarding the globe technique (e.g., the fact that the black globe technique cannot handle different absorption values in the different radiation wavelength domains and absorbs more short-wave radiation than the human body; the globe thermometer has not enough time in outdoors to reach its equilibrium value). Therefore, the comparisons will be presented in a "two-step" way as follows:

- We deal separately with the question of the reference shapes (spherical shape vs. standing man shape) based only on the six-directional technique and analyze the

**Table 1** Instrumentation used in the Taiwanese and the Hungarian parallel (globe—six-directional) measurement campaigns (accuracy of the parameters is shown in parentheses)

	Huwei, Taiwan → correction database (9 days from 2010-12-03 to 2011-04-09)	Szeged, Hungary → validation database (7 days from 2013-09-02 to 2013-12-03)
$K_i$ & $L_i$	Lateral fluxes: NR01 net radiometers, HUKSEFLUX vertical fluxes: CNR-1 net radiometer, Kipp & Zonen	Rotatable CNR-2 net radiometer, Kipp & Zonen (rotated in new position in every 3 min)
$T_g$	Standard black globe with a Pt100 DIN-IEC 751 sensor ( $\pm 0.15$ °C at 0 °C)	Standard black globe with a DCP D100089 HiTemp sensor ( $\pm 1$ °C at $-10$ – $50$ °C)
$T_a$	Pt100 1/3 DIN with forced ventilation, LSI-Lastem ( $\pm 0.1$ °C at 0 °C)	Thermocap sensor as part of a WXT 520, Vaisala ( $\pm 0.25$ °C at 0 °C; $\pm 0.3$ °C at 20 °C; $\pm 0.4$ °C at 40 °C)
RH	From wet and dry bulb temperatures Pt100 1/3 DIN with forced ventilation, LSI-Lastem (2 % at 15–45 °C)	Humicap sensor as part of a WXT 520, Vaisala ( $\pm 3$ % at 0–90 %; $\pm 5$ % at 90–100 %)
$v$	Cups and vane anemometer, LSI-Lastem (1.5 % at 0–3 m/s; 1 % at >3 m/s)	Ultrasonic anemometer—part of a WXT 520, Vaisala ( $\pm 0.3$ m/s or $\pm 3$ %—whichever is greater)

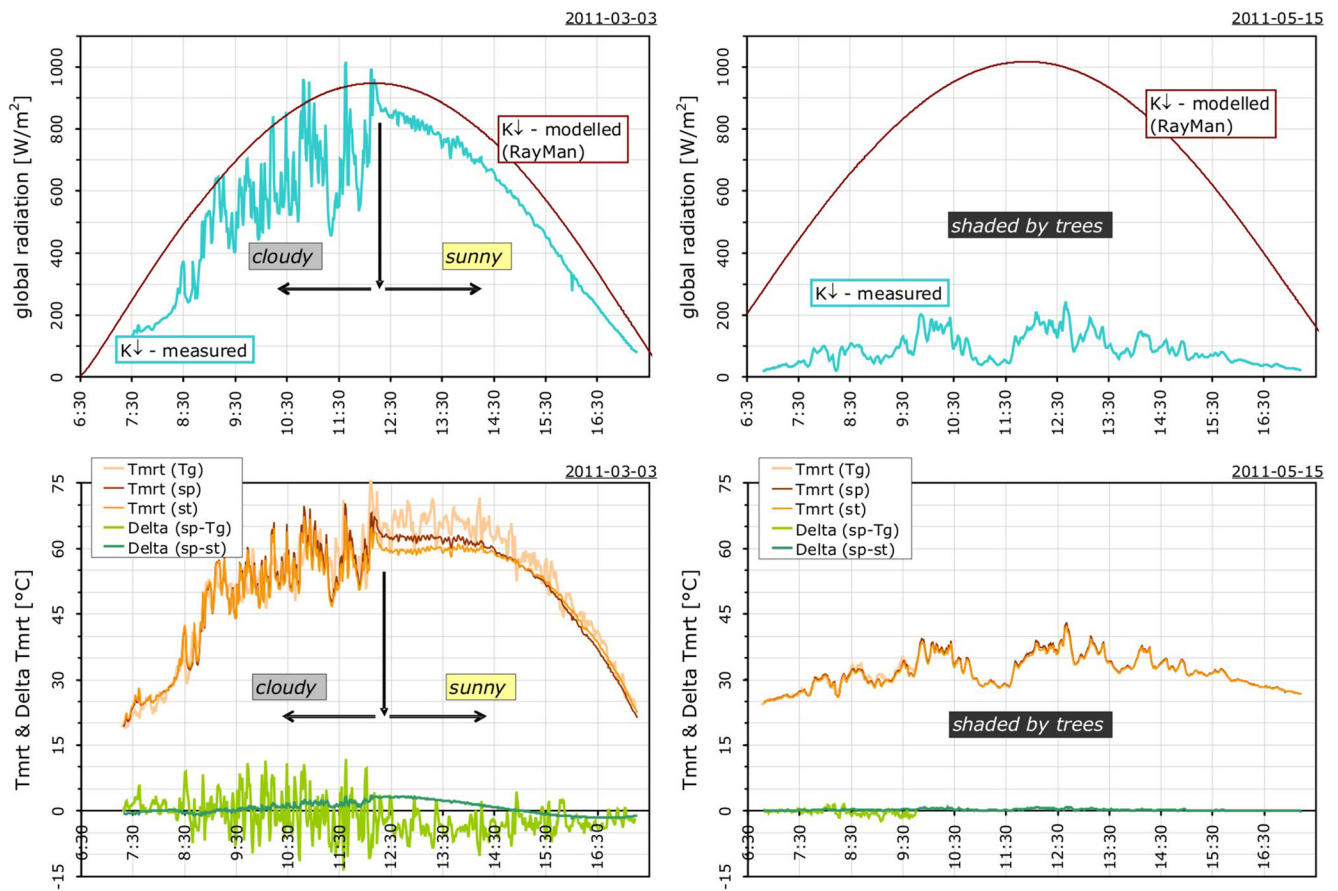


**Fig. 1** Demonstration of the main characteristics of the different  $T_{mrt}$  values, i.e., their differences during cloudy and clear sky conditions when the SVF is near to 1 (*left part*) and when the sensors are totally shaded (*right part*)—two from the 12 Taiwanese measurement days as example

**Table 2** Distributional statistics of some parameters included in the Taiwanese correction database

$N=3,833$	Minimum	Maximum	Mean	Std. deviation	Skewness (std. error: 0.040)	Kurtosis (std. error: 0.079)
$K\downarrow$	0	1,017	522	226.893	-0.429	-0.818
RH	33.3	97.4	63.0	14.4055	0.009	-0.672
$T_a$	12.9	27.4	19.8	3.0309	-0.157	-0.278
$T_g$	11.9	45.2	29.6	6.5850	-0.311	-0.183
$v$	0.5	3.5	1.8	0.6983	0.519	-0.444
$T_{mrt}(st)$	9.2	70.9	51.1	11.8131	-1.305	1.039
$T_{mrt}(sp)$	8.4	71.7	51.5	12.5254	-1.172	0.659
$T_{mrt}(T_g)$	7.1	82.5	54.1	13.7251	-1.082	0.681
PET(st)	7.2	46.7	27.6	7.4314	-0.425	-0.163
PET(sp)	7.0	47.1	27.8	7.7101	-0.405	-0.280
PET( $T_g$ )	6.7	48.4	29.0	8.4710	-0.328	-0.371
$T_{mrt}(sp)-T_{mrt}(st)$	-3.4	4.6	0.4	1.5367	-0.097	-0.129
$T_{mrt}(sp)-T_{mrt}(T_g)$	-18.9	13.9	-2.6	3.7337	-0.111	0.960
$T_{mrt}(st)-T_{mrt}(T_g)$	-19.8	14.5	-3.0	4.2621	-0.481	0.596
PET(sp)-PET(st)	-1.4	2.1	0.2	0.6689	0.180	-0.211
PET(sp)-PET( $T_g$ )	-8.3	7.4	-1.2	1.7309	-0.288	1.037
PET(st)-PET( $T_g$ )	-9.0	7.7	-1.4	1.9828	-0.650	0.752

differences between the calculated  $T_{\text{mrt}}(\text{st})$  and  $T_{\text{mrt}}(\text{sp})$  values and the caused differences in terms of the PET index.

- After that, taking into account a more similar reference shape, we analyze the differences emerging from the different techniques, i.e., the black globe technique and the six-directional technique using identical directional weighting factors for all radiation flux densities— $T_{\text{mrt}}(T_g)$  and  $T_{\text{mrt}}(\text{sp})$  values and the caused differences in terms of the PET index.

After that, we will look for correction functions to improve the fit between the  $T_{\text{mrt}}(T_g)$  and the six-directional  $T_{\text{mrt}}$  values using the same Taiwanese Correction Database.

## 2.2 The Hungarian “validation database”

The effectiveness of the determined relationships will be tested also on an independent *Validation Database from Hungary* (Table 1). Here, the parallel globe and six-directional measurements took place during the daylight period of 7 days in the year 2013 in the official meteorological garden of Szeged (46.25° N, 20.15° E) without considerable horizon limitation (SVF ca. 1). From the measurement-technological point of view, the most important difference between the Hungarian and Taiwanese measurement series relates to the recording of the radiation flux densities (Table 1). While in Taiwan all necessary flux densities were measured simultaneously by three net radiometers, the Hungarian group applied a rotatable net radiometer which was turned in a new position every 3 min. Therefore, the temporal resolution of the six-directional  $T_{\text{mrt}}$  values in Hungary is coarser.

During the detailed preliminary analyses of these data, we identified the time periods when the fit of the different  $T_{\text{mrt}}$  values was almost perfect and the  $T_{\text{mrt}}(T_g)$  data do not need further correction. These situations coincided with longer overcast sky conditions. Because of this founding, and because the Taiwanese Correction Database included only sunny and cloudy conditions, we performed the validations with a filtered Hungarian Database, namely, after that the overcast situations had been removed from them. Finally, the Hungarian Validation Database includes 2,194 datasets from 7 measurement days.

## 3 Taiwanese results

### 3.1 The role of the different reference shapes and techniques—“status quo”

First of all, we demonstrate the differences between the measurement techniques as well as reference shapes. In contrast to

the fully shaded situation, the different techniques resulted in quite different  $T_{\text{mrt}}$  values during sunny and cloudy (but not overcast!) conditions (Fig. 1).

The role of the reference shape and the Sun’s elevation angle is obvious during clear weather when we focus on the differences between the  $T_{\text{mrt}}(\text{sp})$  and  $T_{\text{mrt}}(\text{st})$  values (Fig. 1). During high solar altitude, the spherical reference shape got more radiation load ( $T_{\text{mrt}}(\text{sp})$  was higher), while in the late afternoon, the role of the lateral directions became more important; therefore,  $T_{\text{mrt}}(\text{st})$  was higher. These findings are in accordance with the statements of earlier studies (Thorsson et al. 2007; Mayer et al. 2008). It is worth noticing that the different reference shapes caused relatively low differences compared to the different techniques, i.e., they were always lower than 4 °C in absolute value while the differences between the  $T_{\text{mrt}}(\text{sp})$  and  $T_{\text{mrt}}(T_g)$  sometimes exceeded the 10 °C in absolute value. It is also notable that the effect of reference shapes was even smaller during cloudy situations (Fig. 1).

Considering the deviations between the  $T_{\text{mrt}}(\text{sp})$  and  $T_{\text{mrt}}(T_g)$  values, we can see different patterns during the cloudy and during the clear parts of the day as well. When it was sunny, the  $T_{\text{mrt}}(T_g)$  values were systematically bigger, i.e., the globe technique overestimated the real value of the  $T_{\text{mrt}}$  because the black painting of the globe absorbed too much short-wave radiation. The other characteristic is that the  $T_{\text{mrt}}(T_g)$  fluctuated intensively despite the unobstructed sky conditions and smooth (real)  $T_{\text{mrt}}$  curve. This is because the  $T_g$  value was influenced by not only the radiative heat exchange processes between the globe and the environment but also the convective heat exchanges. In spite of the fact that the wind velocity and air temperature were incorporated into the  $T_{\text{mrt}}(T_g)$  equation to eliminate the effect of the convective part, the globe had not enough time to reach the equilibrium  $T_g$  (which would be required for the reliable calculations) because of the rapidly variable outdoor wind velocity. Incorporating non-equilibrium  $T_g$  and contemporaneous wind velocity into the equation results in uncertain, highly fluctuating  $T_{\text{mrt}}(T_g)$ , similar to that we can see in the study of Thorsson et al. (2007) as well.

In the cloudy part of the day, we cannot observe the systematical overestimation of the globe technique; however, the fluctuation of the  $[T_{\text{mrt}}(\text{sp}) - T_{\text{mrt}}(T_g)]$  difference was even bigger (Fig. 1). The reason for this pattern is that there were two rapidly changing environmental factors which influenced the  $T_g$  inside the globe: the real  $T_{\text{mrt}}$  (which fluctuated because of the cloudy sky) and the wind velocity. And again, the globe’s response time was too long to react immediately to these swift changes, which resulted in remarkably different  $T_{\text{mrt}}(T_g)$  values compared to the real ones.

As a next step, we consider all data from the Taiwanese correction database. The  $T_{\text{mrt}}$  values based on the six-directional technique, namely the  $T_{\text{mrt}}(\text{st})$  and  $T_{\text{mrt}}(\text{sp})$ , ranged mainly between [10; 70 °C] with quite similar frequency

distribution and mostly fell in the [24; 64 °C] domain (Fig. 2, Table 2). The  $T_{\text{mrt}}(\text{st})$  and  $T_{\text{mrt}}(\text{sp})$  had exactly the same median (55.6 °C) and mode (60 °C) values, while the arithmetic mean was slightly higher in the case of the spherical reference shape (51.1 and 51.5 °C). Although with almost the same mode (61 °C), the globe technique resulted in obviously different distribution of  $T_{\text{mrt}}$  values with lower skewness and kurtosis, meaning more symmetric and less centered distribution (Fig. 2, Table 2). Mean (54.1 °C), median (57.6 °C), and the 95 % percentile values (70.2 °C) were all higher than those in the case of the six-directional technique. The generally higher values of  $T_{\text{mrt}}(T_g)$  can be attributed to the excessive short-wave radiation absorption of the black globe, and the wider range is because of the too long response time of the globe which resulted in highly unsteady, fluctuating  $T_{\text{mrt}}(T_g)$  values during the variable outdoor (sky and/or wind field) conditions.

The difference between the differently weighted six-directional  $T_{\text{mrt}}$  values [ $T_{\text{mrt}}(\text{sp}) - T_{\text{mrt}}(\text{st})$ ] was every time within the  $\pm 5$  °C domain (ranged from  $-3.4$  to  $4.6$  °C) and almost in half of the cases (48 %) in the  $\pm 1$  °C domain (Fig. 3, Table 2). Of the cases, 64 % resulted in a higher  $T_{\text{mrt}}(\text{sp})$  than  $T_{\text{mrt}}(\text{st})$ . Using these  $T_{\text{mrt}}$  values to calculate the PET index, the reference-shape-based differences resulted in a narrower *Delta PET* [ $PET(\text{sp}) - PET(\text{st})$ ] distribution (from  $-1.4$  to  $2.1$  °C). Less than 15 % of the data were out of the  $\pm 1$  °C range, and less than 1 % exceeded 2 °C.

Considering different techniques, the differences were much greater and indicated usually higher values in the case of the globe technique (Fig. 3). Even with the same reference shape [ $T_{\text{mrt}}(\text{sp}) - T_{\text{mrt}}(T_g)$ ], one quarter of the data differed more than 5 °C from the six-directional  $T_{\text{mrt}}$ , and this proportion was nearly one-third when we compared the  $T_{\text{mrt}}(T_g)$  to the “standing man”  $T_{\text{mrt}}(\text{st})$ . In terms of PET, 78 % [ $PET(\text{sp}) - PET(T_g)$ ] and 73 % [ $PET(\text{st}) - PET(T_g)$ ] of the cases fell into the  $[-2.5; 2.5$  °C] *Delta PET* domain.

Based on the finding that the reference shape (standing shape vs. spherical shape) did not cause serious deviations between the values of the bioclimate indices, thereafter it seems to be enough to focus on the differences between the techniques, i.e., the  $T_{\text{mrt}}(\text{sp})$  and  $T_{\text{mrt}}(T_g)$  values. In the following sections, we seek to find simple correction functions to lower the differences between the different techniques, i.e., to make the *Delta T<sub>mrt</sub>* distributions more centralized around 0—more symmetric and with less standard deviation compared to the original distributions in Fig. 3.

### 3.2 Direct correction between the different $T_{\text{mrt}}$ values

First, a direct regression analysis was conducted between the  $T_{\text{mrt}}(T_g)$  values as input variable (regressor) and  $T_{\text{mrt}}(\text{sp})$  values as the wished output variable (regressand). The presented regressions could be considered somewhat innovative compared to the earlier published comparisons as, besides the linear regression, a second degree function was also fitted to the data pairs. The analysis was conducted based on the whole data package on the one hand and separately for sunny (clear sky) and cloudy situations on the other hand. The sunny/cloudy separation was based not on automated techniques but on the visual analysis of the time series of  $K_{\downarrow}$  and  $T_{\text{mrt}}$  values on all of the measurement days. One example of the separation can be seen in Fig. 1.

The results of the direct  $T_{\text{mrt}}(\text{sp})$  vs.  $T_{\text{mrt}}(T_g)$  regression are summarized in Fig. 4 and Table 3. The quadratic regressions always gave better  $R^2$  values, especially in the sunny group. Later (in the “Discussion” section), we will apply the two equations in Table 3 highlighted with yellow as *direct correction technique* to improve the fit between the  $T_{\text{mrt}}$  values originating from the globe technique and the desired  $T_{\text{mrt}}(\text{sp})$ .

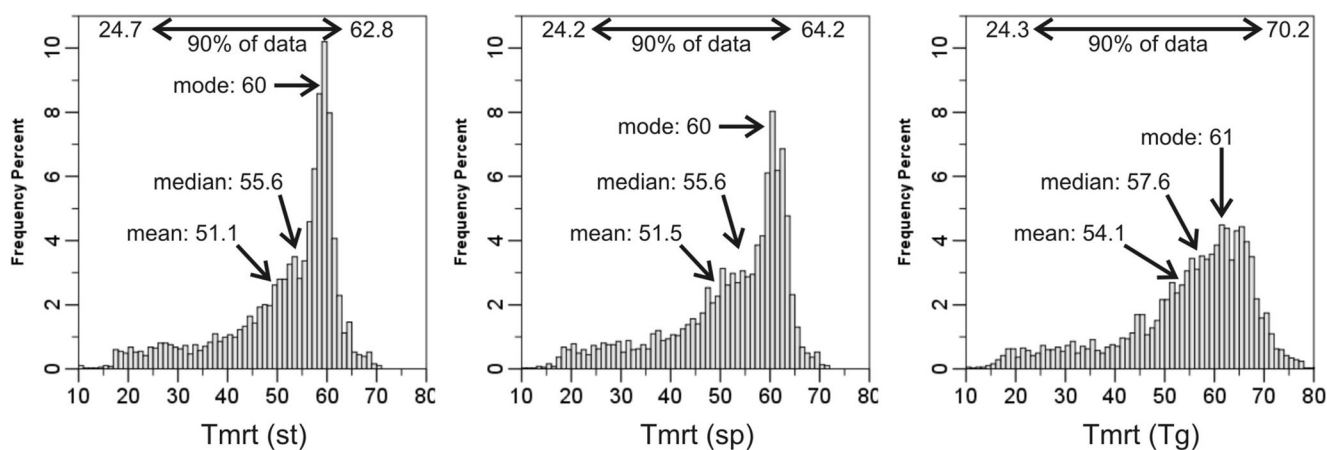


**Fig. 2** Some distributional statistics (mean, median, mode as well as the 5 and 95 % percentiles) of the different  $T_{\text{mrt}}$  values (to determine the mode the  $T_{\text{mrt}}$  values were rounded to integers)

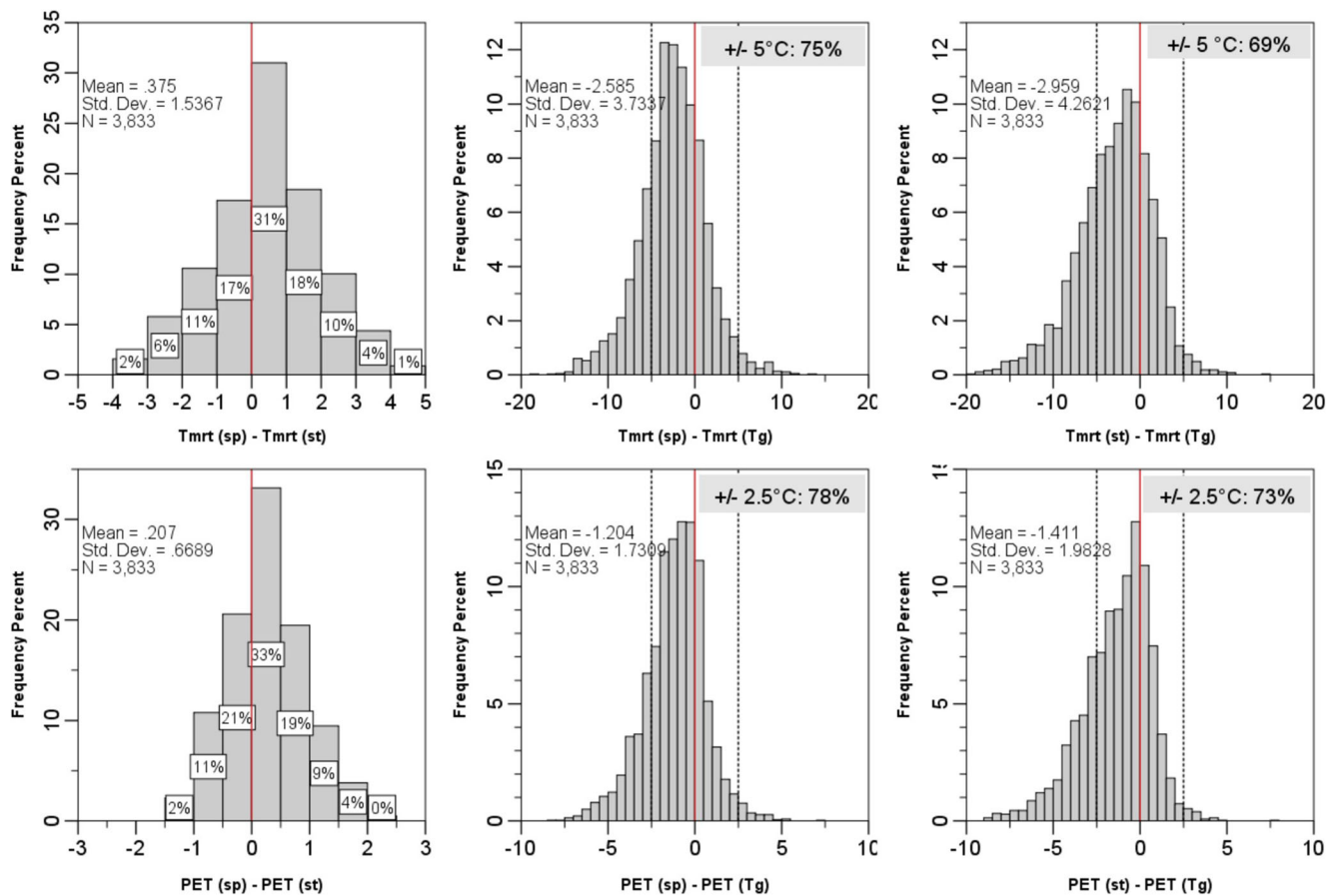


Fig. 3 Frequency distribution of the different  $\Delta T_{mrt}$  and the corresponding  $\Delta$  PET values

### 3.3 Indirect correction

In the second case, we were looking for easily accessible parameters which are closely related to the  $\Delta T_{mrt}$  [ $T_{mrt}(sp) - T_{mrt}(T_g)$ ] values to be able to correct the  $T_{mrt}(T_g)$  values indirectly. The concept behind this somewhat sophisticated method is that we want to apply

the corrections later on other databases, which cover different ranges in terms of the different basic variables and calculated variables; therefore, it is possible that an indirect way would result in better corrected  $T_{mrt}(T_g)$  values.

When looked for parameters which determine greatly the differences between the  $T_{mrt}$  values based on the

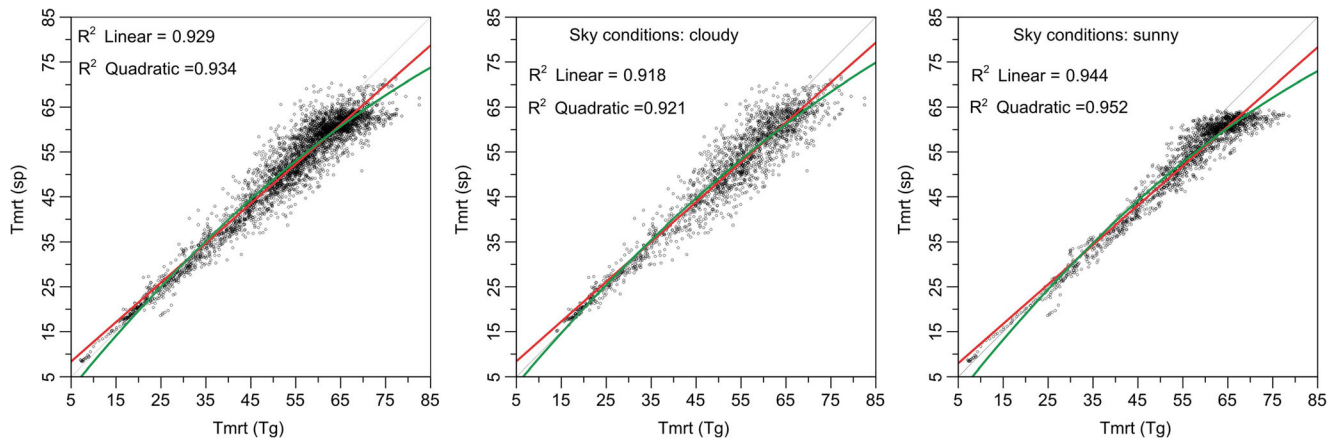


Fig. 4 Direct regression between the  $T_{mrt}(sp)$  and  $T_{mrt}(T_g)$  values



**Table 3** Direct regression functions between the  $T_{\text{mrt}}(\text{sp})$  and  $T_{\text{mrt}}(T_g)$  values

	$R^2$	Regression function— $y: T_{\text{mrt}}(\text{sp}); x: T_{\text{mrt}}(T_g)$
Whole database ( $N=3,833$ )	0.929	$y=3.936+8.794 \cdot 10^{-1} x$
	0.934	$y=-3.849+1.255 x-4.028 \cdot 10^{-3} x^2$
Cloudy conditions ( $N=1,949$ )	0.918	$y=3.957+8.866 \cdot 10^{-1} x$
	0.921	$y=-2.706+1.212 x-3.521 \cdot 10^{-3} x^2$
Sunny conditions ( $N=1,884$ )	0.944	$y=3.545+8.791 \cdot 10^{-1} x$
	0.952	$y=-5.291+1.300 x-4.458 \cdot 10^{-3} x^2$

same reference shape but on different measurement techniques [ $T_{\text{mrt}}(\text{sp})-T_{\text{mrt}}(T_g)$ ], there was a basic criteria—the potential regressor should be obtained easily during globe thermometer measurements or generated easily after the measurements. Therefore, we analyzed the relationships with the following:

- $v, T_a, T_g, T_g-T_a$  (as they are obviously available during globe measurements),
- the  $K\downarrow$  global radiation (measured by the up-faced pyranometer on the site in our case, but usually it is relatively easy to obtain from the nearby meteorological station),
- average  $K\downarrow$  from the previous 10 min (based on the idea that the globe response time is longer and such a value may have greater effect),
- the elevation value of the Sun (obtained from the RayMan model based on the geographical coordinates, date and time) and some trigonometric functions of the elevation.

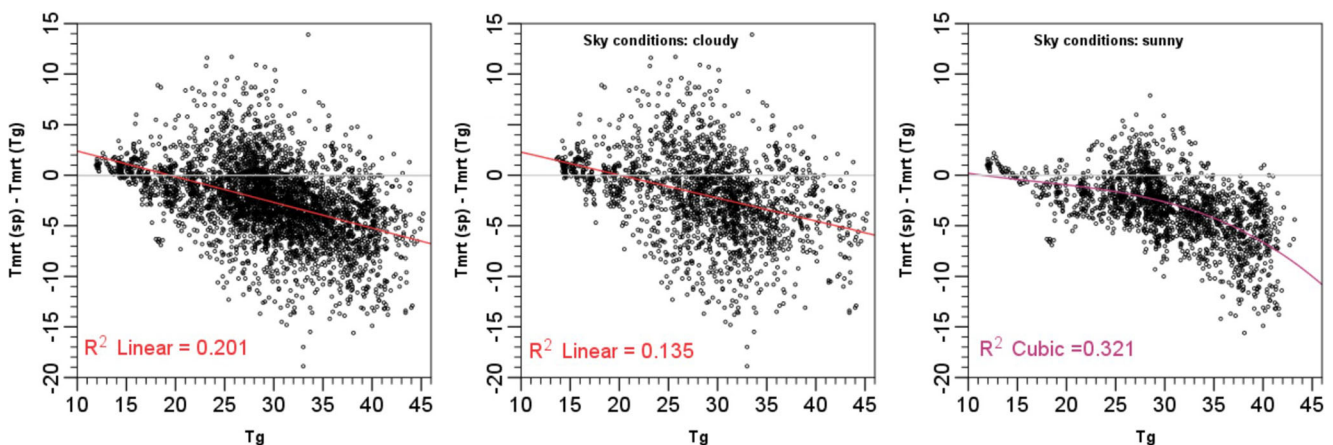
As the  $T_{\text{mrt}}(T_g)$  values fluctuated greatly with time (e.g., Fig. 1), their differences from the  $T_{\text{mrt}}(\text{sp})$  values resulted in a great scatter in the function of every parameter and caused relatively low  $R^2$  values in spite of the fact that

the relationships were significant (at 0.0001 level). The best  $R^2$  values emerged when the regressor was the  $T_g$  itself (Fig. 5, Table 4). In the case of the whole database and during cloudy conditions, the  $R^2$  values were the same regardless of the degree of the fitted curve; therefore, we suggest the simplest linear regression. In the case of clear sky conditions, however, the third degree function seemed considerably better than the others.

#### 4 Discussion

This section discusses the effectiveness of the suggested direct and indirect correction techniques on the original Taiwanese database and on an independent Hungarian database as a validation. The directly corrected  $T_{\text{mrt}}$  was calculated simply by substituting the original  $T_{\text{mrt}}(T_g)$  values into the yellow-highlighted equations presented in Table 3. To get the indirectly corrected  $T_{\text{mrt}}(T_g)$ , we calculated firstly the supposed differences between the  $T_{\text{mrt}}(\text{sp})$  and  $T_{\text{mrt}}(T_g)$  values based on the yellow equations of Table 4 using the  $T_g$  as regressor, then we added this calculated Delta value to the original  $T_{\text{mrt}}(T_g)$ .

The effectiveness of the correction methods will be discussed on the one hand by displaying the scatter plot diagrams of the original and the corrected  $T_{\text{mrt}}(T_g)$  values as a function of the desired  $T_{\text{mrt}}(\text{sp})$ . The closer is the fitted linear line to the  $x=y$  relationship and the smaller is the scatter of the data, the better is the method. On the other hand, we show the frequency distribution of the Delta  $T_{\text{mrt}}$  values. The more centralized is the distribution around zero, the better is the correction method (Figs. 6–7).

**Fig. 5** Regression between the [ $(T_{\text{mrt}}(\text{sp})-T_{\text{mrt}}(T_g))$ ] and  $T_g$

**Table 4** Regression functions between the  $[(T_{mrt}(sp)-T_{mrt}(T_g))]$  and  $T_g$

	$R^2$	Regression function— $y: T_{mrt}(sp)-T_{mrt}(T_g);$ $x: T_g$
Whole database	0.201	$y=4.939-2.544 \cdot 10^{-1} x$
Cloudy conditions	0.135	$y=4.571-2.278 \cdot 10^{-1} x$
Sunny conditions	0.321	$y=2.537-3.506 \cdot 10^{-1} x+1.456 \cdot 10^{-2} x^2-2.879 \cdot 10^{-4} x^3$

4.1 The efficiency of the applied correction methods on the Taiwanese data

Based on the scatter plots, both correction techniques have improved the fit between the  $T_{mrt}(T_g)$  and the  $T_{mrt}(sp)$  values; the relationship moved obviously closer to the desired  $x=y$  linear as well as the determination coefficient became slightly greater (Fig. 6). The scatter of the data lowered a bit more when applying the direct correction, and 88 % of the cases become in the  $\pm 5^\circ\text{C}$  Delta  $T_{mrt}$  domain in both methods. It is important to notice, however, that below  $20^\circ\text{C}$   $T_{mrt}$ s the direct method caused greater differences than in the original

situation. The main reason behind this is that the Correction Database contained less low  $T_{mrt}$  values (only 5 % of the cases was lower than  $24^\circ\text{C}$ ; Fig. 2), and the resulted correction equations were driven mainly by the higher  $T_{mrt}$  domain (Fig. 4). Therefore, when using the direct correction method, we suggest to use it only in the cases when  $T_{mrt}(T_g)$  is above  $20^\circ\text{C}$ , while under this value, it seems to be more appropriate to leave the original values of  $T_{mrt}(T_g)$  without modification until the time somebody repeats the analyses on a more evenly distributed or on a normally distributed  $T_{mrt}$  database.

4.2 Validation of the correction functions with an independent database

In the case of the Hungarian database, 51 % of the Delta  $T_{mrt}$  values fell into the  $\pm 5^\circ\text{C}$  domain originally, which is a substantially lower proportion than in the Taiwanese situation. While the correction functions improved the fit between the  $T_{mrt}(T_g)$  and the  $T_{mrt}(sp)$  values, this improvement was not so considerable: only 56 % (5 % increase) and 57 % (6 % increase) of the cases fell into the  $\pm 5^\circ\text{C}$  Delta  $T_{mrt}$  range after

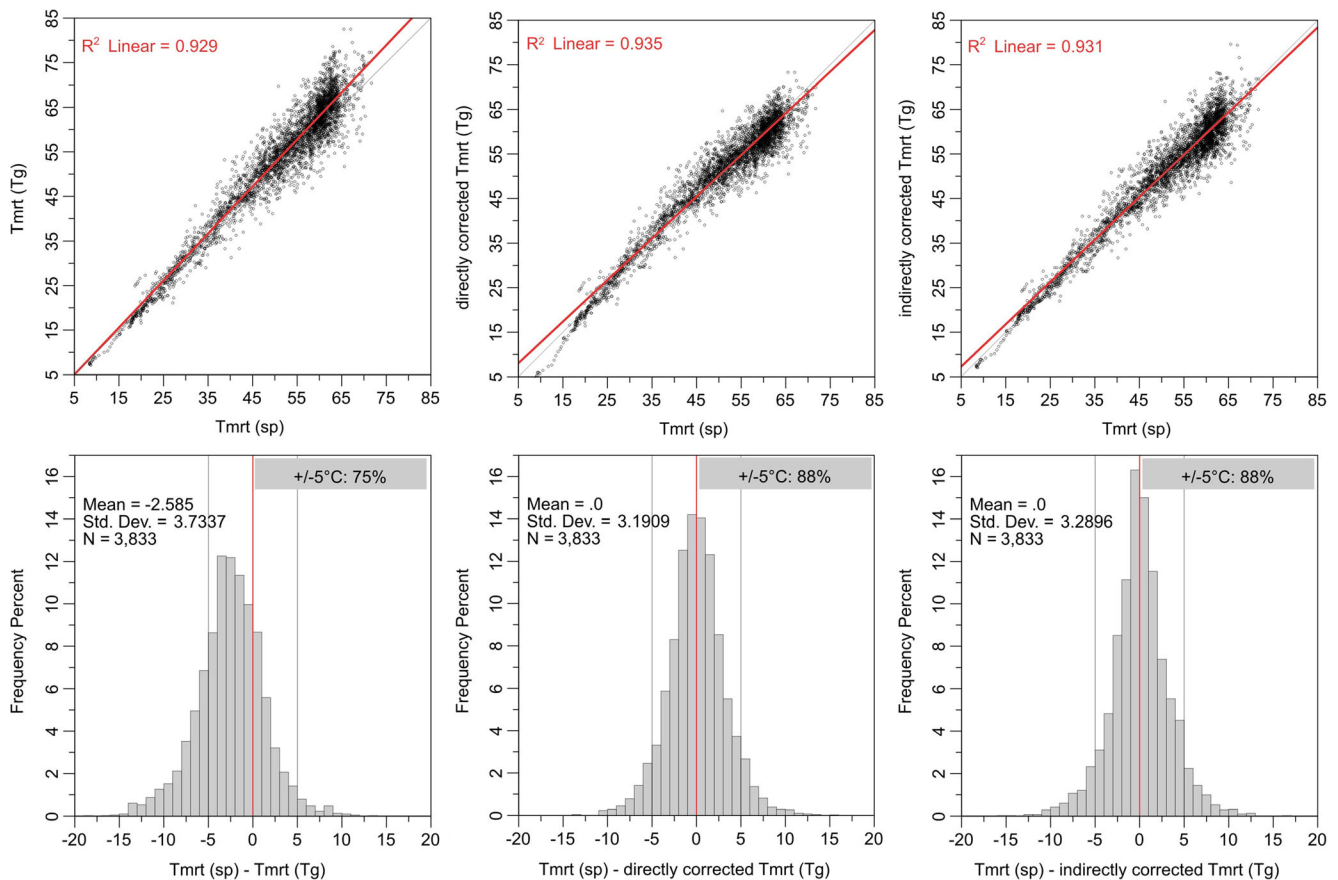


**Fig. 6** Demonstration of the different correction methods' efficiency in improving the fit between the  $T_{mrt}(T_g)$  and the  $T_{mrt}(sp)$  using the Taiwanese database (from left to right—original data pairs, direct correction, and indirect correction)

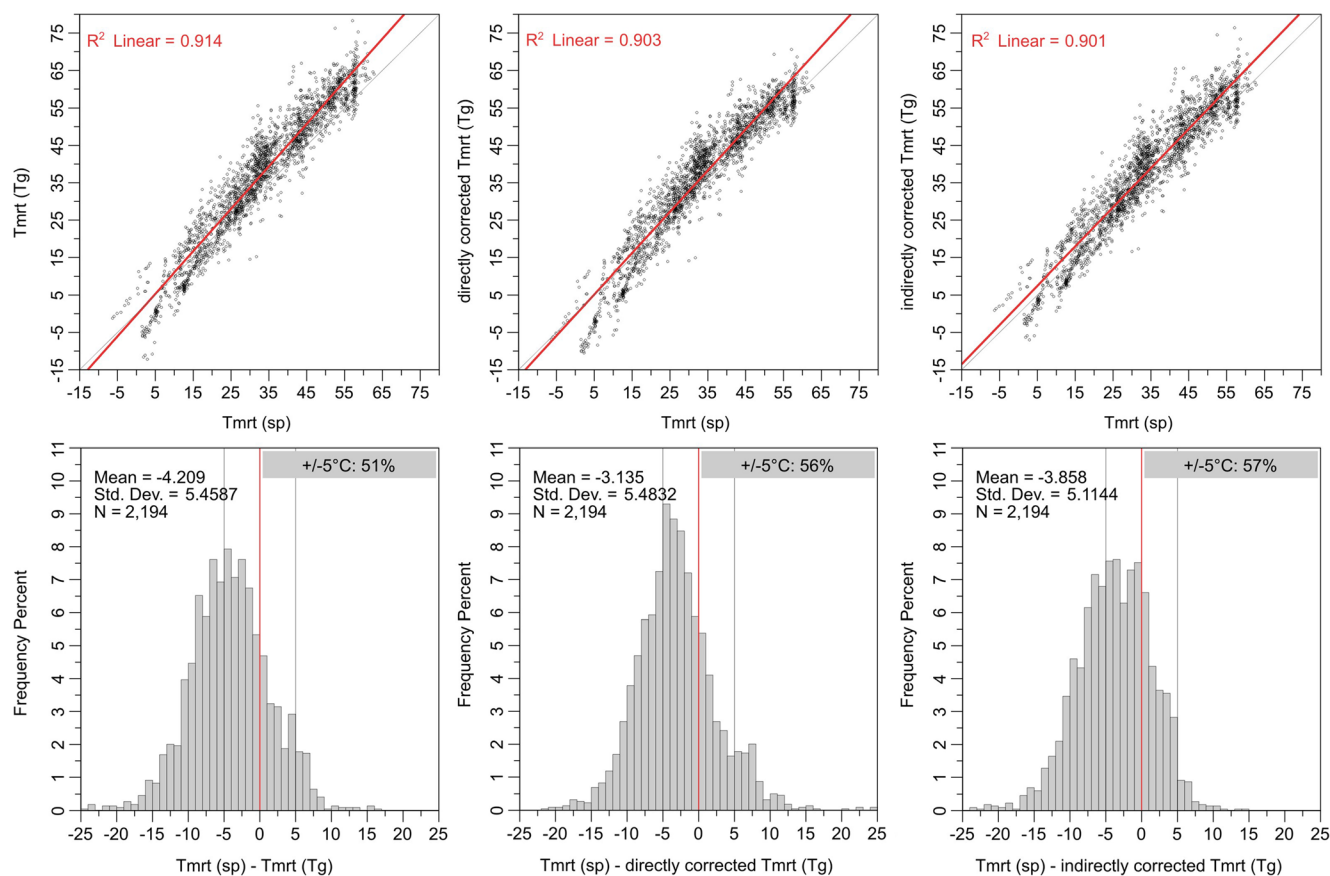


**Fig. 7** Demonstration of the different correction methods' efficiency on the Hungarian database (from left to right—original data pairs, direct correction, and indirect correction)

the direct and indirect corrections, respectively; moreover, the  $R^2$  values became slightly poorer (Fig. 7).

The possible explanation is that the frequency distributions of the basic (and calculated) parameters were totally different in Hungary than those in Taiwan because of the following:

- the Taiwanese data were collected from December to April, while the Hungarian data covered the September–December months of the year;
- the background climate is totally different in the two sites, including, among others, different Sun-path properties (solar elevation, strength of radiation flux densities);
- moreover, while in Taiwan the measurement days were sunny or cloudy, the recordings in Hungary were conducted more often on cloudy or overcast days. Consequently, lower radiation flux densities were measured than they would be on the same days with clearer sky conditions, which associated also lower temperature values.

Based on these findings, we should conclude that it is not recommended to use the recent Taiwanese correction

functions on datasets which have been measured in considerably different geographical/climatic conditions.

## 5 Conclusions

Mean radiant temperature values were calculated and compared to each other in Taiwan based on two popular measurement techniques. In the case of the six-directional technique, two different  $T_{mrt}$  values were applied:  $T_{mrt}(st)$ , which represents the radiation load on a standing man, and  $T_{mrt}(sp)$ , which refers to a spherical reference shape. Moreover,  $T_{mrt}(T_g)$  was obtained through the globe thermometer technique applying the standard black globe.

- (1) The first objective of this study was to describe the differences between the mentioned  $T_{mrt}$  values and quantify what a difference can be assumed in terms of a bioclimate index (PET) incorporating those  $T_{mrt}$  values. Comparing  $T_{mrt}(st)$  and  $T_{mrt}(sp)$ , the differences were always in the  $\pm 5$  °C domain and caused only very small differences between the PET(st) and PET(sp): 85 % of the

data were inside the  $\pm 1$  °C Delta PET range, and less than 1 % exceeded 2 °C. Of the cases, 75 % fell into the  $\pm 5$  °C Delta  $T_{\text{mrt}}$  range when we compared the  $T_{\text{mrt}}(\text{sp})-T_{\text{mrt}}(T_g)$  data pairs and only 69 % when the  $T_{\text{mrt}}(\text{st})-T_{\text{mrt}}(T_g)$  data pairs. The corresponding frequencies, when the Delta PET values were in the  $\pm 2.5$  °C domain, were 78 % [PET(sp)-PET( $T_g$ )] and 73 % [PET(st)-PET( $T_g$ )].

- (2) The second research objective was to make the already existing Taiwanese outdoor thermal comfort projects with black globe-based  $T_{\text{mrt}}(T_g)$  values comparable to other databases which involve six-directional  $T_{\text{mrt}}$ . In line with this aim, simple correction functions were determined to improve the fit between the  $T_{\text{mrt}}$  values from the two techniques. The corrections were conducted directly between the  $T_{\text{mrt}}(T_g)$  and  $T_{\text{mrt}}(\text{sp})$  values and also indirectly, i.e., by using the values of  $T_g$  to reduce the differences between  $T_{\text{mrt}}(\text{sp})$  and  $T_{\text{mrt}}(T_g)$ . Both correction methods resulted in considerable improvement and reduced the differences between the  $T_{\text{mrt}}(\text{sp})$  and the  $T_{\text{mrt}}(T_g)$  values. Originally, only 75 % of the data were in the  $\pm 5$  °C Delta  $T_{\text{mrt}}$  range, but using either the direct or the indirect correction functions, this proportion increased to 88 %. As the Taiwanese Correction Database of parallel globe and six-directional measurements was compiled to fit to the atmospheric conditions of the former Taiwanese outdoor thermal comfort project (FIOT project), the resulted correction functions can be used in the future to recalculate the  $T_{\text{mrt}}(T_g)$  values of the FIOT project when it is necessary to compare them with other databases including six-directional  $T_{\text{mrt}}$ .
- (3) Validations with an independent database from Hungary revealed that it is not suggested to apply the resulted correction functions under totally different background climate. However, other research groups can follow and develop further the suggested methodology to find relative easy corrections between different  $T_{\text{mrt}}$  techniques. Outdoor validation of the (black) globe technique is necessary, but it needs local measurement series under meteorological conditions which characterize properly the given location as well as the time periods when people spend their time usually in the open air.

**Acknowledgment** The authors would express a special thank for the sponsorship of the Research Center for the Humanities and Social Sciences at the National Chung Hsing University.

## References

- Abdel-Ghany AM, Al-Helal IM, Shady MR (2013) Human thermal comfort and heat stress in an outdoor urban arid environment: a case study. *Adv Meteorol*, Article ID 693541
- Ali-Toudert F (2005) Dependence of the outdoor thermal comfort on street design in hot and dry climate. *Ber Meteor Inst Albert-Ludwigs-Univ Freiburg* 15:224p
- Ali-Toudert F, Mayer H (2007) Thermal comfort in an east–west oriented street canyon in Freiburg (Germany) under hot summer conditions. *Theor Appl Climatol* 87:223–237
- Ali-Toudert F, Djenane M, Bensalem R, Mayer H (2005) Outdoor thermal comfort in the old desert city of Beni-Isguen, Algeria. *Clim Res* 28:243–256
- Andrade H, Alcoforado MJ (2008) Microclimatic variation of thermal comfort in a district of Lisbon (Telheiras) at night. *Theor Appl Climatol* 92:225–237
- Andrade H, Alcoforado MJ, Oliveira S (2011) Perception of temperature and wind by users of public outdoor spaces: relationships with weather parameters and personal characteristics. *Int J Biometeorol* 55:665–680
- ASHRAE (2001) Chapter 14—measurements and instruments. In: *ASHRAE fundamentals handbook*. American Society for Heating Refrigerating and Air-Conditioning Engineers, Atlanta:14.28–14.29
- Bedford T, Warner CG (1934) The globe thermometer in studies of heating and ventilation. *J Hyg (Lond)* 34:458–473
- Chen H, Ooka R, Harayama K, Kato S, Li X (2004) Study on outdoor thermal environment of apartment block in Shenzhen, China with coupled simulation of convection, radiation and conduction. *Energ Buildings* 36:1247–1258
- Deb C, Ramachandraiah A (2010) Evaluation of thermal comfort in rail terminal location in India. *Build Environ* 45:2571–2580
- Deb C, Ramachandraiah A (2011) A simple technique to classify urban locations with respect to human thermal comfort: proposing the HXG scale. *Build Environ* 46:1321–1328
- Fanger PO (1972) *Thermal comfort*. McGraw Hill Book Co, New York, p 244
- Gulyás Á, Unger J, Matzarakis A (2006) Assessment of the microclimatic and thermal comfort conditions in a complex urban environment: modelling and measurements. *Build Environ* 41:1713–1722
- Holst J, Mayer H (2010) Urban human-biometeorology: investigations in Freiburg (Germany) on human thermal comfort. *Urban Climate News* 38:5–10
- Höppe P (1992) Ein neues Verfahren zur Bestimmung der mittleren Strahlungstemperatur in Freien. *Wetter und Leben* 44:147–151
- Höppe P (1999) The physiological equivalent temperature—a universal index for the biometeorological assessment of the thermal environment. *Int J Biometeorol* 43:71–75
- Hwang RL, Lin TP (2007) Thermal comfort requirements for occupants of semi-outdoor and outdoor environments in hot-humid regions. *Archit Sci Rev* 50:357–364
- Hwang RL, Lin TP, Cheng MJ, Lo JH (2010) Adaptive comfort model for tree. Shaded outdoors in Taiwan. *Build Environ* 45:1873–1879
- Hwang RL, Lin TP, Matzarakis A (2011) Seasonal effects of urban street shading on long-term outdoor thermal comfort. *Build Environ* 46:863–870
- ISO (1985) ISO Standard 7726. Thermal environments—instruments and methods for measuring physical quantities.
- ISO (1998) ISO Standard 7726. Ergonomics of the thermal environments—instruments for measuring physical quantities.
- Jendritzky G (1993) The atmospheric environment—an introduction. *Experientia* 49:733–738
- Jendritzky G, Nübler W (1981) A model analysing the urban thermal environment in physiologically significant terms. *Arch Met Geoph Biokl B* 29:313–326
- Kántor N, Unger J (2010) Benefits and opportunities of adopting GIS in thermal comfort studies in resting places: an urban park as an example. *Landscape Urban Plan* 98:36–46
- Kántor N, Égerházi L, Unger J (2012a) Subjective estimations of thermal environment in recreational urban spaces—part 1: investigations in Szeged, Hungary. *Int J Biometeorol* 56:1075–1088

- Kántor N, Unger J, Gulyás Á (2012b) Subjective estimations of thermal environment in recreational urban spaces—part 2: international comparison. *Int J Biometeorol* 56:1089–1101
- Kántor N, Matzarakis A, Lin TP (2013) Daytime relapse of the mean radiant temperature based on the six-directional method under unobstructed solar radiation. *Int J Biometeorol*, DOI 10.1007/s00484-013-0765-5
- Krüger EL, Rossi FA (2011) Effect of personal and microclimate variables on observed thermal sensation from a field study in southern Brazil. *Build Environ* 46:690–697
- Krüger EL, Minella FO, Rasia F (2011) Impact of urban geometry on outdoor thermal comfort and air quality from field measurements in Curitiba, Brazil. *Build Environ* 46:621–634
- Lee H, Holst J, Mayer H (2013) Modification of human-biometeorologically significant radiant flux densities by shading as local method to mitigate heat stress in summer within urban street canyons. *Adv Meteorol* 06:1–13
- Lin TP (2009) Thermal perception, adaptation and attendance in a public square in hot and humid regions. *Build Environ* 44:2017–2026
- Lin TP, Matzarakis A, Hwang RL (2010) Shading effect on long-term outdoor thermal comfort. *Build Environ* 45:213–221
- Lin TP, de Dear R, Hwang RL (2011) Effect of thermal adaptation on seasonal outdoor thermal comfort. *Int J Climatol* 31:302–312
- Lindberg F, Grimmond CSB (2011) The influence of vegetation and building morphology on shadow patterns and mean radiant temperatures in urban areas: model development and evaluation. *Theor Appl Climatol* 105:311–323
- Lindberg F, Holmer B, Thorsson S (2008) SOLWEIG 1.0—modelling spatial variations of 3D radiant fluxes and mean radiant temperature in complex urban settings. *Int J Biometeorol* 52:697–713
- Matzarakis A, Rutz F, Mayer H (2007) Modelling radiation fluxes in simple and complex environments—application of the RayMan model. *Int J Biometeorol* 51:323–334
- Matzarakis A, Rutz F, Mayer H (2010) Modelling radiation fluxes in simple and complex environments: basics of the RayMan model. *Int J Biometeorol* 54:131–139
- Mayer H (1993) Urban bioclimatology. *Experientia* 49:957–963
- Mayer H (2008) KLIMES—a joint research project on human thermal comfort in cities. *Ber Meteor Inst Albert-Ludwigs-Univ Freiburg* 17:101–117
- Mayer H, Höppe P (1987) Thermal comfort of man in different urban environments. *Theor Appl Climatol* 38:43–49
- Mayer H, Holst J, Dostal P, Imbery F, Schindler D (2008) Human thermal comfort in summer within an urban street canyon in Central Europe. *Meteorol Z* 17:241–250
- Ng E, Cheng V (2012) Urban human thermal comfort in hot and humid Hong Kong. *Energy Buildings* 55:51–65
- Nikolopoulou M, Lykoudis S (2006) Thermal comfort in outdoor urban spaces: analysis across different European countries. *Build Environ* 41:1455–1470
- Nikolopoulou M, Lykoudis S (2007) Use of outdoor spaces and microclimate in a Mediterranean urban area. *Build Environ* 42:3691–3707
- Nikolopoulou M, Steemers K (2003) Thermal comfort and psychological adaptation as a guide for designing urban spaces. *Energy Buildings* 35:95–101
- Nikolopoulou M, Baker N, Steemers K (2001) Thermal comfort in outdoor urban spaces: understanding the human parameter. *Sol Energy* 70:227–235
- Oliveira S, Andrade H (2007) An initial assessment of the bioclimatic comfort in an outdoor public space in Lisbon. *Int J Biometeorol* 52:69–84
- Pearlmutter D, Jiao D, Garb Y (2014) The relationship between bioclimatic thermal stress and subjective thermal sensation in pedestrian spaces. *Int J Biometeorol*, DOI 10.1007/s00484-014-0812-x
- Shashua-Bar L, Tsiros IX, Hoffman M (2012) Passive cooling design options to ameliorate thermal comfort in urban streets of a Mediterranean climate (Athens) under hot summer conditions. *Build Environ* 57:110–119
- Spagnolo J, de Dear RJ (2003) A field study of thermal comfort in outdoor and semi-outdoor environments in subtropical Sydney Australia. *Build Environ* 38:721–738
- Streilung S, Matzarakis A (2003) Influence of single and small clusters of trees on the bioclimate of a city: a case study. *J Arboriculture* 29:309–316
- Tan CL, Wong NH, Jusuf SK (2013) Outdoor mean radiant temperature estimation in the tropical urban environment. *Build Environ* 64:118–129
- Tan CL, Wong NH, Jusuf SK (2014) Effects of vertical greenery on mean radiant temperature in the tropical urban environment. *Landscape Urban Plan* 127:52–64
- Thorsson S, Lindqvist M, Lindqvist S (2004) Thermal bioclimatic conditions and patterns of behaviour in an urban park in Göteborg, Sweden. *Int J Biometeorol* 48:149–156
- Thorsson S, Lindberg F, Holmer B (2007) Different methods for estimating the mean radiant temperature in an outdoor urban setting. *Int J Climatol* 27:1983–1993
- VDI (1998) Methods for the human-biometeorological assessment of climate and air hygiene for urban and regional planning. Part I: climate. VDI 3787, Part 2. Beuth, Berlin, 29p
- Vernon HM (1930) The measurement of radiant heat in relation to human comfort. *J Physiol* 70, Proc, 15p
- Walton D, Dravitzki V, Donn M (2007) The relative influence of wind, sunlight and temperature on user comfort in urban outdoor spaces. *Build Environ* 42:3166–3175